Cyclodextrins
Циклодекстрины

Макрогетероциклы
http://macroheterocycles.isuct.ru

Paper
Статья

Molecular DFT Investigation on the Inclusion Complexation of Benzo[a]pyrene with γ−Cyclodextrin

Nadia Mesri,[a,b@] Youghourta Belhocine,[c] Nabil Messikh,[c] Adlane Sayede,[d] and Benali Mouffok[a]

[a]Laboratoire Synthèse de l'Information Environnementale (LSIE), Faculté des Sciences Exactes, Université Djillali Liabès, 22000 Sidi Bel-Abbès, Algeria.
[b]Département du TC Sciences et Techniques, Faculté des Sciences et Technologie, Université Mustapha Stambouli, 29000 Mascara, Algeria
[c]Department of Petrochemical and Process Engineering, Faculty of Technology, 20 August 1955 University of Skikda, 21000 Skikda, Algeria
[d]UMR 8181 Unité de Catalyse et de Chimie du Solide (UCCS), France
@Corresponding author E-mail: mesri.nadia@univ-mascara.dz, a.mesri.nadia@gmail.com

The complexation process between benzo[a]pyrene (BaP) and γ-cyclodextrin (γ-CD) was computationally studied using DFT methodology. Several initial configurations of the interaction of BaP with γ-CD were explored to determine the most stable inclusion complex. According to the calculated complexation energies, the BaP/γ-CD complex is found to be the most favorable energetically when the BaP guest is totally entrapped into γ-CD cavity. The inclusion process involving the encapsulation of two guests BaP in the cavity of γ-CD is also thermodynamically favored. Van der Waals interactions play a determinant role in stabilizing BaP/γ-CD and 2BaP/γ-CD complexes.

Keywords: γ-Cyclodextrin, benzo[a]pyrene, inclusion complex, DFT calculations, Van der Waals interactions.

Молекулярное DFT−исследование комплексообразования включения бензо[a]пирена с γ−циклодекстрином

Н. Месри,[a,b@] Ю. Белхосин,[c] Н. Мессих,[c] А. Сайеде,[d] Б. Муффок[a]

[a]Факультет точных наук, Университет Джиллали Лябес, 22000 Сиди Бел-Аббес, Алжир
[b]Факультет науки и технологий, Университет Мустафы Стамбули, 29000 Маскара, Алжир
[c]Кафедра нефтехимии и технологического проектирования технологического факультета, 20 августа 1955 г. Университет Скикды, 21000 Скикда, Алжир
[d]Отдел твердотельного катализа и химии UMR 8181 (UCCS), Франция
@E-mail: mesri.nadia@univ-mascara.dz, a.mesri.nadia@gmail.com

Процесс комплексообразования между бензо[a]пиреном (BaP) и γ-циклодекстрином (γ-CD) был изучен с использованием DFT расчетов. Было исследовано несколько начальных конфигураций взаимодействия BaP с γ-CD, чтобы определить наиболее стабильный комплекс включения. Согласно рассчитанным энергиям комплексообразования, комплекс BaP/γ-CD оказывается более энергетически стабилен в случае, когда гость BaP полностью захвачен в полость γ-CD. Процесс включения, в который вовлечена инкапсуляция двух гостей BaP в полость γ-CD, также термодинамически благоприятен. Ван-дер-Ваальсовы взаимодействия играют определяющую роль в стабилизации комплексов BaP/γ-CD и 2BaP/γ-CD.

Ключевые слова: γ-Циклодекстрин, бензо[a]пирен, комплекс включения, DFT расчеты, Ван-дер-Ваальсовы взаимодействия.

Introduction

Benzo[a]pyrene (BaP) belongs to the class of polycyclic aromatic hydrocarbons (PAHs), which are formed during the incomplete combustion of organic matter.[1,2] They are ubiquitous pollutants of major concern because of their significant toxicity to humans,[3–5] ecotoxicity, carcinogenicity, mutagenicity and effects on reproductive ability.[6–9]

Benzo[a]pyrene is a byproduct of incomplete combustion or pyrolysis of organic materials;[6,10] it was characterized and identified at the beginning of the 1930s when Cook, Hewett and Heiger succeeded to synthesize it.[11] The crystalline form of BaP was originally reported by John Iball in 1936,[12] and already at that time its acute toxicity and high carcinogenicity were well known. In the human body, BaP is metabolized to highly reactive species (diol epoxide, quinone or radical cations) which damage DNA leading to cancer; it is the most active carcinogen.[13,14] Major routes of exposure are via inhalation and food intake. Chronic BaP exposure has been associated with the development of various human cancers, including lung, breast and liver cancer; it is classified in Group 1 (carcinogenic to humans) by the International Agency for Research on Cancer (IARC).[15]

Benzo[a]pyrene is also considered as the prototypical PAH, an indicator for PAH contamination with the highest toxicity equivalent factor (TEF) that made it a reference in the toxicity[16] (Scheme 1). The toxic equivalency factor (TEF) makes it possible to evaluate the toxicity of PAHs that have poor toxicological data on the carcinogenicity with quantitative estimates of their carcinogenic potency expressed relative to that of BaP, this allows to analyze their presence in food webs and to attribute a biological significance to their concentrations measured in tissues;[17,18] the presence of benzo[a]pyrene has been identified in a wide range of environmental and combustion-related samples such as cigarette smoke, sediment, air particulate, water, coal tar, crude oil, and diesel particulate,[19,20] and tend to persist in the environment partly and accumulate in soils due to its high hydrophobicity and its strong adsorption onto the soil organic matter, these properties make biodegradation or chemical treatments of BaP very difficult.[21,22]

Among the methodologies developed to extract, treat or analyze BaP and other PAHs are the use of cyclodextrins (CDs);[23,24] that are cyclic oligomers composed of six, seven or eight glucopyranose units which are commonly available in three types α- (alpha), β- (beta) and γ- (gamma) and presenting enclosed cavities approximately of 4.7–5.3, 6.0–6.5, and 7.5–8.3 Å in diameter, respectively. The external part of the cyclodextrins is hydrophilic whereas the interior cavity is hydrophobic enabling them to entrap guest molecules in their molecular cavities, thus allowing remarkable effects in stabilizing and solubilizing lipophilic unstable substances without the formation of chemical bonds and without changing their structure; such physical interaction can be considered as an encapsulation of substances at a molecular scale via non-covalent interactions.[25]

These inclusion systems by encapsulation have allowed cyclodextrins to be widely used in various fields such as pharmaceuticals (vectorization of active ingredients), food technology and cosmetics (aroma protection against oxidation, light and heat, controlled release of fragrances), agriculture (encapsulation of insecticides), chemical analysis (separation method, chromatography, *etc.*), catalysis (biphasic catalysis), textiles and environmental sciences (water treatment, cleaning of polluted soils, air analysis, *etc.*).[26–29]

The inclusion of BaP by cyclodextrin hosts and their derivatives has been subject to some studies in the literature[30–34] that were dedicated to the improvement of BaP biodegradation, however, most of these studies focused on the use of β-cyclodextrin (β-CD) or its derivatives as a host due to its availability, price and cavity size suitable for a broad range of guest molecules.

In this context, the experimental work of Patonay *et al.*[33] regarding the possible formation of inclusion complexes between BaP and α-, β-, and γ-cyclodextrin showed that the formation constant is larger for BaP/γ-CD than for BaP/α-CD and BaP/β-CD complexes. It is also found that BaP forms 1:1 inclusion complex with γ-CD, however, it is less likely for γ-CD to accommodate two guest BaP molecules inside its cavity, however, the spectroscopic binding studies carried out by woodberry *et al.*[34] suggested the possible formation of 2:1 guest:host inclusion complex of BaP metabolites in γ-CD.

In the present investigation, the inclusion complex process between BaP and γ-CD was explored by employing density functional theory (DFT) calculations.

Computational Methods

The starting molecular structure of γ-CD was taken from the crystal structure of uncomplexed γ-cyclodextrin determined by X-ray diffraction.[35] The BaP molecule was drawn with Avogadro (version 1.2.0) software.[36] Both structures of γ-CD and BaP were subjected to geometry optimization at DFT/B97-D3BJ/def2-svp level of theory with ORCA program.[37,38] Frequency calculations were performed to characterize the structures as minimum points on the potential energy surface. The optimized structures were then used to build the inclusion models. The process of inclusion is represented in Figure 1, where the center of γ-CD cavity was defined as the center of the whole system (z = 0 Å) and the BaP guest passes through the cavity of γ-CD from –8 Å to +8 Å along the z-axis with a step of 1 Å. The minimum-energy configurations were identified according to the method of Liu *et al.*[39] For each step, the geometry of the complex was fully optimized using ORCA program in water solvent with the CPCM model[40] at B97-D3BJ/def2-svp level of theory[41–44] without assuming any symmetry constraints; a geometrical counterpoise correction[45] (gCP) for basis set superposition error (BSSE) in the def2-SVP basis was applied, as well as the resolution of identity approximation[46,47] (RI) and fine integration grids (Grid5 for SCF iterations and Grid6 for the final energy). All the calculations were carried out on Intel Core I5 8600K processor personal computer having 16 GB memory, the average calculation time of full geometry optimization for each configuration was about 2.5 days.

The complexation energies (ΔE) were computed by the equation (1) in order to evaluate energetically the inclusion process between BaP and γ-CD in their final optimized geometries:

$$\Delta E = E_{complex} - (E_{BaP} + E_{\gamma\text{-CD}}), \qquad (1)$$

where $E_{complex}$, E_{BaP} and $E_{\gamma\text{-CD}}$ are respectively the total energy of the complex, the free optimized BaP and the free optimized γ-CD.

The most stable structure among the calculated ones corresponds to the conformation with the lowest total energy value for both A and B models.
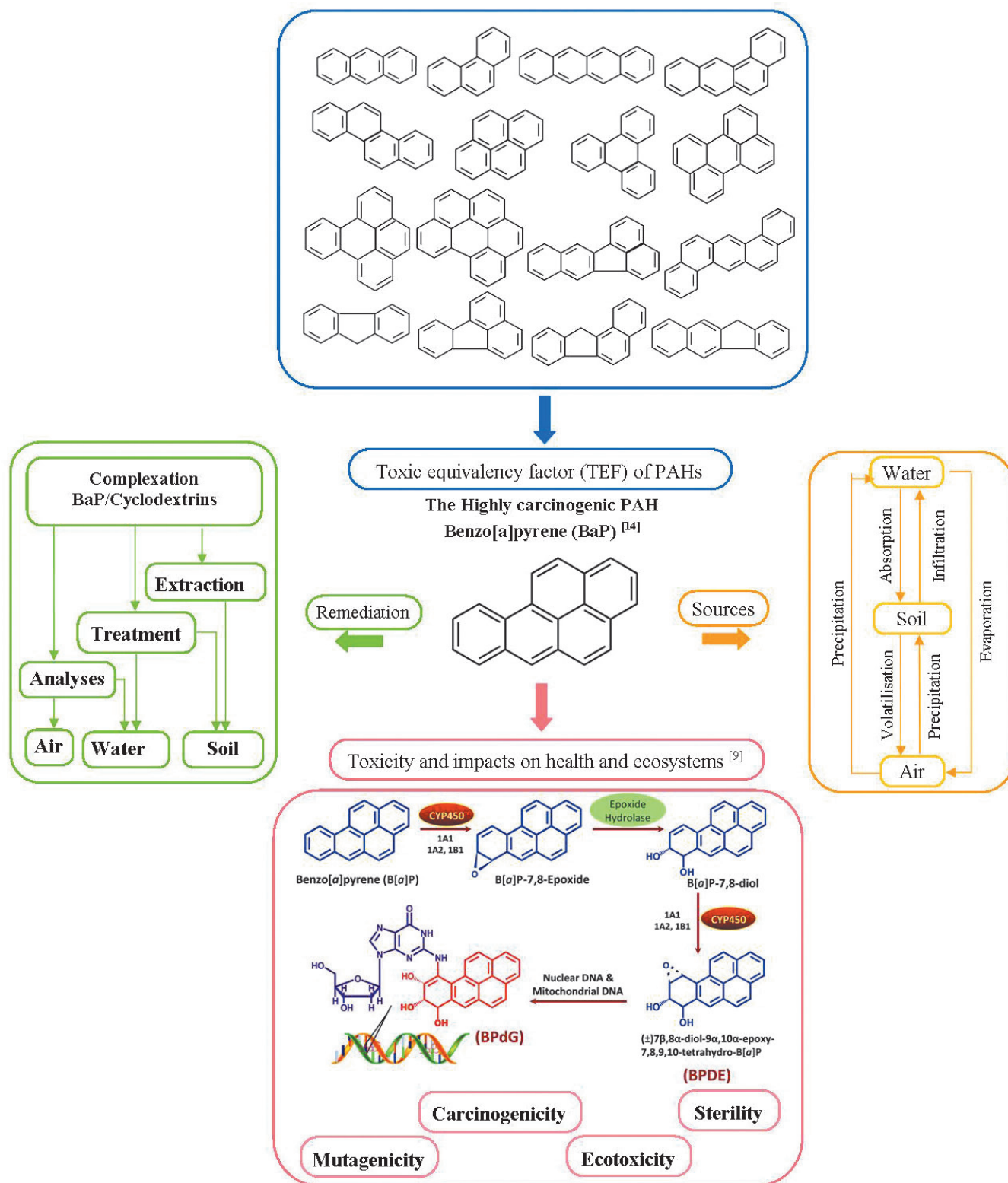
Scheme 1. Toxic and health effects of benzo[a]pyrene on organisms and environment.

Results and Discussion

Complexation Energy Computations

The computed complexation energies of the most stable conformations corresponding to the minimum-energy structures found for A and B models are reported in Table 1.

The complexation energy values are negative, implying a favorable thermodynamic process, and they are found to be more negative when the BaP penetrates the γ-CD cavity more deeply. Indeed, the energy of the complexation increases negatively as the BaP guest approaches the center of γ-CD cavity, suggesting that weak intermolecular forces are behind the stability of the formed complexes.[49–51]
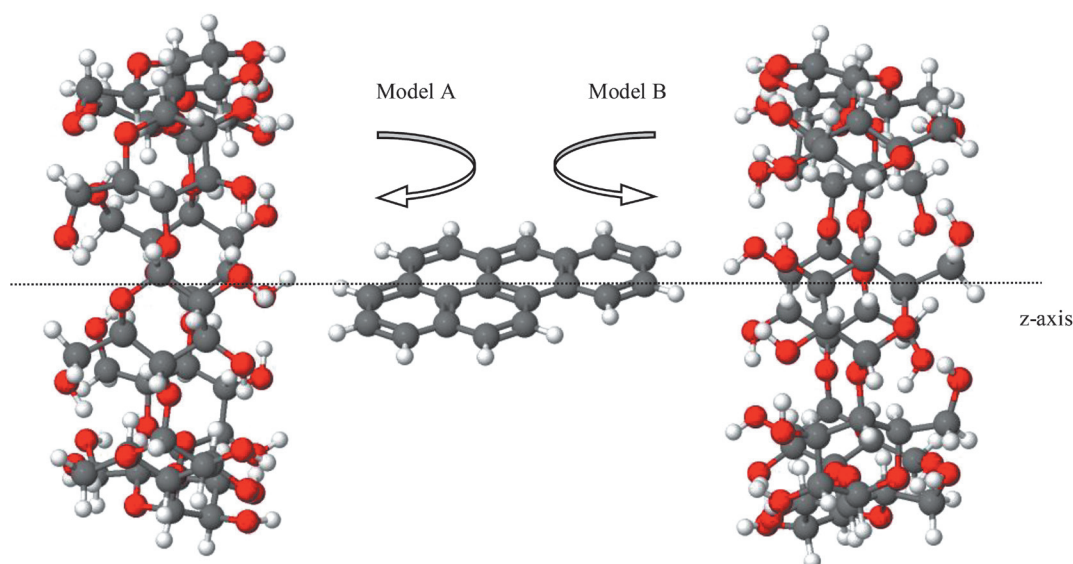
Figure 1. Illustration of the inclusion models of BaP in γ-CD visualized by Jmol viewer applet.[48] Color code of atoms (grey for C, red for O and white for H).

The most stable conformations for both A and B models are located at z = 0 Å (Table 1), the corresponding complexation energies are respectively –61.71 and –48.13 kJ/mol, with an energy difference of 13.58 kJ/mol in favor of A model.

Table 1. Computed complexation energies (kJ/mol) of BaP/γ-CD at B97-D3BJ/def2-SVP level in CPCM water model

| Initial configurations (Å)	BaP/γ-CD (kJ/mol)	Initial configurations (Å)	BaP/γ-CD (kJ/mol)
Model A		Model B	
–8	–13.60	–8	–29.10
–7	–21.00	–7	–3.42
–6	–24.75	–6	–26.39
–5	–27.99	–5	–31.61
–4	–32.72	–4	–35.09
–3	–39.44	–3	–37.14
–2	–43.34	–2	–43.35
–1	–47.03	–1	–36.39
0	**–61.71**	0	**–48.13**
+1	–46.13	+1	–42.73
+2	–45.79	+2	–42.78
+3	–41.20	+3	–40.49
+4	–39.91	+4	–41.58
+5	–28.67	+5	–25.45
+6	–28.16	+6	–18.53
+7	–8.89	+7	–15.73
+8	–2.17	+8	–11.16

Electronic and Sensing Properties of γ-CD towards BaP

The calculated quantum chemical parameters[52–54] such as frontier molecular orbitals (HOMO and LUMO), HOMO-LUMO energy gap, dipole moment (μ)[55] and the percentage of variation of HOMO–LUMO gap $|\Delta E_g|$[56,57] can be useful for rationalizing the electronic properties of both γ-CD and the formed inclusion complex BaP/γ-CD. The computed values for these quantities are listed in Table 2.

Table 2. Computed chemical parameters of γ-CD and BaP/γ-CD complex.

Chemical Parameters	γ-CD	BaP/γ-CD
Dipole moment μ (D)	14.00	14.05
HOMO (eV)	–5.89	–4.75
LUMO (eV)	0.39	–2.57
Gap E_g (eV)	6.28	2.18
Gap variation $|\Delta E_g|$ (%)	–	65.29

The results reported in Table 2 show that the HOMO and LUMO levels are shifted to upper and lower energies, respectively upon the formation of the inclusion complex BaP/γ-CD, leading to a significant decrease of the HOMO–LUMO energy gap from 6.28 eV for γ-CD to 2.18 eV for the complex BaP/γ-CD. The percentage variation in HOMO–LUMO gap $|\Delta E_g|$ is about 65.3 %. Thus, the electrical properties of BaP/γ-CD complex are significantly affected by the complexation process; therefore, γ-CD can be used as a sensor for electrical detection of BaP. Once the complex is formed, a negligible variation in the global dipole moment is observed (14.00 D for γ-CD and 14.05 D for BaP/γ-CD), suggesting that electric dipole moment does not appear to influence the complexation process.
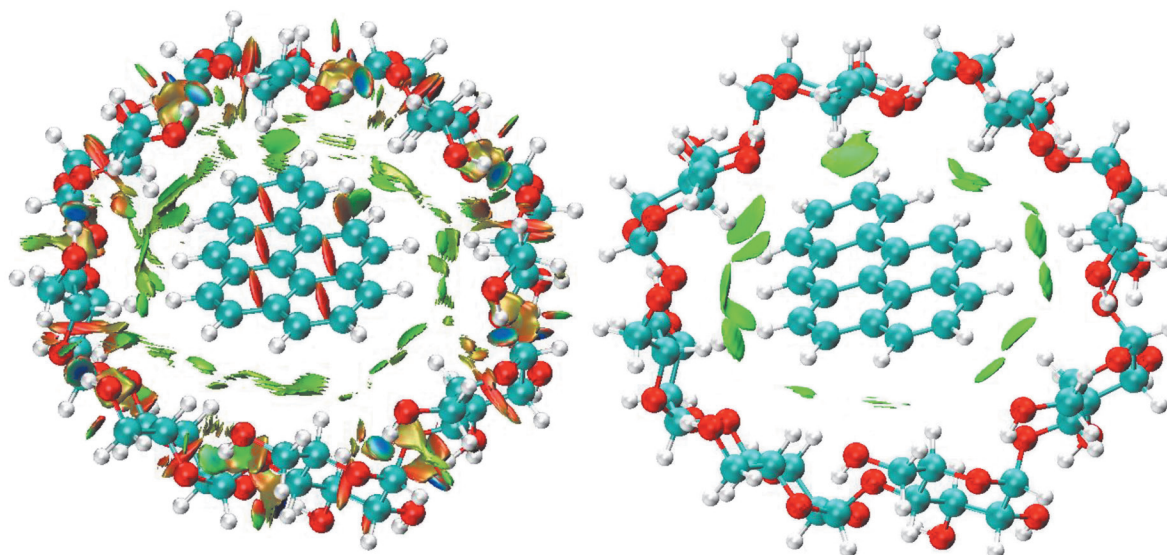
Figure 2. RDG (left isovalue 0.7 a.u.) and IGM (right isovalue 0.003 a.u.) isosurfaces of BaP/γ-CD complex.
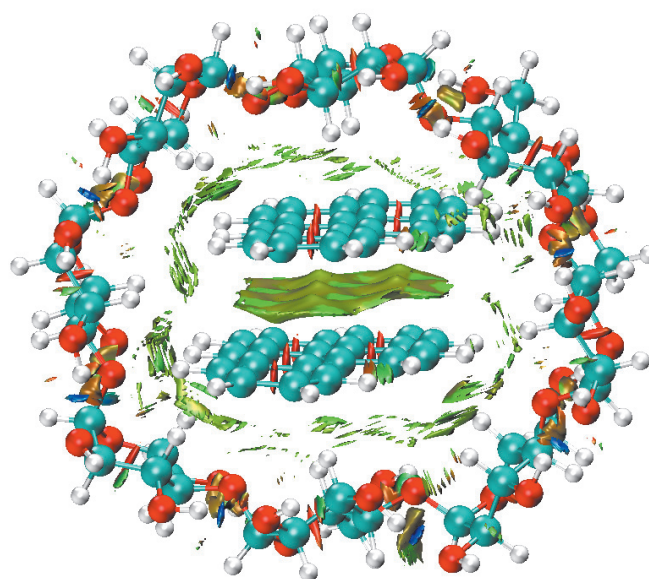
Non-covalent Interaction Analysis

In order to gain a better understanding of the driving forces that govern the complexation of BaP with γ-CD, a non-covalent interaction (NCI) analysis[58] through the reduced density gradient (RDG)[59] and independent gradient model based on Hirshfeld partition of molecular density (IGMH)[60] was performed by Multiwfn program.[61] VMD software[62] was used for three-dimensional visualization of RDG and IGM isosurfaces of BaP/γ-CD complex that are illustrated in Figure 2. The isosurfaces are colored depending on the type of the interaction, thus green, red and blue colors are assigned respectively to weak Van der Waals interactions, steric repulsion and strong electrostatic interactions.

The analysis of intramolecular interactions through the RDG isosurface in Figure 2 (left) revealed the presence of intramolecular hydrogen bonding (blue color) and steric repulsion (red color) occurring in γ-CD whereas steric repulsion (red rice grain-shaped) is dominant within the aromatic rings of BaP. The IGM isosurface (Figure 2 right) identified the intermolecular interactions between γ-CD and BaP and showed that Van der Waals interactions (green color) are solely involved in the formation of the BaP/γ-CD complex.

Formation of 1:2 Host-Guest Inclusion Complex of γ-CD with BaP

To determine theoretically if an inclusion complex can also be formed between γ-CD and two guest BaP molecules, DFT calculations were performed with the same level of theory used for 1:1 host-guest inclusion complex. The calculated complexation energy for 2BaP/γ-CD (–165.17 kJ/mol) indicates the higher probability of formation of an inclusion complex involving the encapsulation of two BaP molecules in the cavity of γ-CD. The non-covalent intra- and intermolecular interactions through RDG isosurface are illustrated in Figure 3. It was found that the inclusion process of two

BaP molecules in γ-CD is largely governed by weak van der Waals interactions indicated by the green or green-brown colors in the RDG isosurface. The BaP guests (dimer) are arranged in a parallel-displaced geometry, contributing, therefore, to energy stabilization of the formed complex. Indeed, the combined effects of π···π stacking as a result of the attraction between the π clouds of the aromatic rings lead to a significant increase in interaction energy between the BaP dimer (–66.97 kJ/mol). Our calculations showed also that the theoretical volume of the γ-CD cavity increased by 15.7 % once the two BaP guests are encapsulated, therefore, due to the conformational flexibility of its structure, γ-CD can accommodate two BaP as guests. The electrical properties of 2BaP/γ-CD complex are more affected if compared with γ-CD and BaP/γ-CD complex, the HOMO and the LUMO are respectively the highest (–4.26 eV)

Figure 3. RDG isosurface (isovalue 0.5 a.u.) of intra- and intermolecular non-covalent interactions in 2BaP/γ-CD complex.

and the lowest (–2.31 eV) in energy and hence the gap is even lower (1.95 eV). The percentage variation in HOMO–LUMO gap $|\Delta E_g|$ for 2BaP/γ-CD complex is about 69 % denoting, therefore, more sensing properties when two BaP molecules are entrapped.

Conclusions

The formation of 1:1 and 1:2 host-guest inclusion complexes of γ-cyclodextrin with benzo[a]pyrene was theoretically investigated by means of DFT calculations. Both 1:1 and 1:2 host-guest complexes are energetically favored due to their negative complexation energies. Van der Waals forces stabilize and govern the intermolecular interactions occurring within BaP/γ-CD and 2BaP/γ-CD complexes. The electrical properties based on the percentage variation of the HOMO–LUMO gap showed that γ-cyclodextrin can serve as a sensor for detecting the presence of benzo[a]pyrene. Our results indicate also the good conformational flexibility of γ-cyclodextrin which allows an increase of its cavity volume by 15.7 % to ensure the inclusion of two benzo[a]pyrene guests.

References

1. Katsoyiannis A., Breivik K. *Environ. Pollut.* **2014**, *184*, 488–494. doi:10.1016/j.envpol.2013.09.028.
2. Zhou H., Wu C., Onwudili J.A., Meng A., Zhang Y., Williams P.T. *Waste Manage.* **2015**, *36*, 136–146. doi:10.1016/j.wasman.2014.09.014.
3. Rengarajan T., Rajendran P., Nandakumar N., Lokeshkumar B., Rajendran P., Nishigaki I. *Asian Pac. J. Trop. Biomed.* **2015**, *5*, 182–189. doi:10.1016/s2221-1691(15)30003-4.
4. Wang, L., Zhang, S., Wang, L., Zhang, W., Shi, X., Lu, X., Li, X. *Int. J. Environ. Res. Public Health.* **2018**, *15*, 607. doi:10.3390/ijerph15040607.
5. Chang Y., Siddens L.K., Heine L.K., Sampson D.A., Yu Z., Fischer K.A., Löhr C.V., Tilton S.C. *Toxicol. Appl. Pharmacol.* **2019**, *379*, 114644. doi:10.1016/j.taap.2019.114644.
6. Chang Y., Huynh C.T.T., Bastin K.M., Rivera B.N., Siddens L.K., Tilton S.C. *Toxicol. In Vitro* **2020**, 104991. doi:10.1016/j.tiv.2020.104991.
7. Bolden A.L., Rochester J.R., Schultz K., Kwiatkowski C.F. *Reprod. Toxicol.* **2017**, *73*, 61–74. doi:10.1016/j.reprotox.2017.07.012.
8. Cathey A.L., Watkins D.J., Rosario Z.Y., Vélez Vega C.M., Loch-Caruso R., Alshawabkeh, A.N., Cordero J.F., Meeker J.D. *Sci. Total Environ.* **2020**, 141581. doi:10.1016/j.scitotenv.2020.141581.
9. Barnes J.L., Zubair M., John K., Poirier M.C., Martin F.L. *Biochem. Soc. Trans.* **2018**, *46*,1213–1224. doi:10.1042/bst20180519.
10. De la Rosa J.M., Sánchez-Martín A.M., Campos P., Miller A.Z. *Sci. Total Environ..* **2019**, *667*, 578–585. doi:10.1016/j.scitotenv.2019.02.421.
11. Cook J.W., Hewett C.L., Hieger I. *J. Chem. Soc.* **1933**, *106*, 395. doi:10.1039/jr9330000395.
12. Phillips D.H. *Nature* *1983*, *303(5917)*, 468–472. doi:10.1038/303468a0.
13. Nebert D.W., Shi Z., Galvez-Peralta M., Uno S., Dragin N. *Mol. Pharmacol.* **2013**, *84*, 304–313. doi:10.1124/mol.113.086637.
14. Honda M., Suzuki N. *Int. J. Environ. Res. Public Health* **2020**, *17*, 1363. doi:10.3390/ijerph17041363.
15. IARC. *IARC. Monogr. Eval. Carcinog. Risks Hum.* **2012**, *100F*, 111–144.
16. Nisbet I.C.T., LaGoy P.K. *Regul. Toxicol. Pharmacol.* **1992**, *16*, 290–300. doi:10.1016/0273-2300(92)90009-x.
17. Petry T., Schmid P., Schlatter C. *Chemosphere* **1996**, *32*, 639–648. doi:10.1016/0045-6535(95)00348-7.
18. Ohiozebau E., Tendler B., Codling G., Kelly E., Giesy J.P., Jones P.D. *Environ. Geochem. Health.* **2016**, *39*, 139–160. doi:10.1007/s10653-016-9815-3.
19. Song Y., Nahrgang J., Tollefsen K.E. *Sci. Total Environ.* **2019**, *653*, 176–189. doi:10.1016/j.scitotenv.2018.10.261.
20. Boente C., Baragaño D., Gallego J. R. *Environ. Pollut.* **2020**, *266*, 115341. doi:10.1016/j.envpol.2020.115341.
21. Choong C.E., Wong K.T., Yoon S.Y., Kim, H., Shin, M., Chang Y.Y., Yang J.K., Kim S.H., Jeon B.H., Yoon Y., Jang M. *J. Clean. Prod.* **2021**, *278*, 123425. doi:10.1016/j.jclepro.2020.123425.
22. Morales P., Cáceres M., Scott F., Díaz-Robles L., Aroca G., Vergara-Fernández A. *Appl. Microbiol. Biotechnol.* **2017**, *101*, 6765–6777. doi:10.1007/s00253-017-8400-8.
23. Veignie E., Rafin C., Landy D., Fourmentin S., Surpateanu G. *J. Hazard. Mater.* **2009**, *168*, 1296–1301. doi:10.1016/j.jhazmat.2009.03.012.
24. Greene L., Elzey B., Franklin M., Fakayode S.O. *Spectrochim. Acta* **2017**, *174*, 316–325. doi:10.1016/j.saa.2016.11.047.
25. Szejtli, J. *Chem. Rev.* **1998**, *98*, 1743–1753. doi:10.1021/cr970022c.
26. Tian B., Xiao D., Hei T., Rui Ping R., Shiyao Huac S., Liuc J. *Polym Int.* **2020**, *69*, 597–603. doi:10.1002/pi.5992.
27. Carneiro S., Costa Duarte F., Heimfarth L., Siqueira Quintans J., Quintans-Júnior L., Veiga Júnior V., Neves de Lima Á. *Int. J. Mol. Sci.* **2019**, *20*, 642. doi:10.3390/ijms20030642.
28. Sayede A., Ponchel A., Filardo G., Galia A., Monflier E. *J. Mol. Struct.* **2006**, *777*, 99–106. doi:10.1016/j.theochem.2006.08.033.
29. Bednarek E., Bociana W., Michalska K. *J. Pharm. Biomed. Anal.* **2019**, *169*, 170–180. doi:10.1016/j.jpba.2019.02.031.
30. Westerberg G., Wiklund L. *J. Pharm. Sci.* **2005**, *94*, 114–119. doi:10.1002/jps.20198.
31. Liu T., Ding K., Guo G., Yang F., Wang L. *Chem Ecol.* **2018**, *34*, 519–531. doi:10.1080/02757540.2018.1462343.
32. Yang M., Wang Y., Wang H. *Electrochim. Acta* **2015**, *169*, 7–12. doi:10.1016/j.electacta.2015.04.057.
33. Patonay G., Warner I.M. *J. Incl. Phenom. Macrocycl. Chem.* **1991**, *11*, 313–322. doi:10.1007/bf01041410.
34. Woodberry R., Ransom S., Chen F.M. *Anal. Chem.* **1988**, *60*, 2621–2625. doi:10.1021/ac00174a017.
35. Harata K. *Bull. Chem. Soc. Jpn.* **1987**, *60*, 2763–2767. doi:10.1246/bcsj.60.2763.
36. Hanwell M.D., Curtis D.E., Lonie D.C., Vandermeersch T., Zurek E., Hutchison G.R. *J. Cheminform.* **2012**, *4*, 17. doi:10.1186/1758-2946-4-17.
37. Neese F., The ORCA program system, Wiley Interdiscip. Rev.: *Comput. Mol. Sci.* **2012**, *2*, 73–78. doi:10.1002/wcms.81.
38. Neese F., Software update: the ORCA program system, version 4.0. *WIREs Comput. Mol. Sci.* **2017**, *8*, e1327. doi:10.1002/wcms.1327.
39. Liu L., Guo Q.X. *J. Incl. Phenom. Macrocycl. Chem.* **2004**, *50*, 95–103. doi:10.1007/s10847-003-8847-3.
40. Takano Y., Houg K.N. *J. Chem. Theory Comput.* **2005**, *1*, 70–77. doi:10.1021/ct049977a.
41. Becke A.D. *J. Chem. Phys.* **1997**, *107*, 8554. doi:10.1063/1.475007.
42. Grimme S., Ehrlich S., Goerigk L. *J. Comput. Chem.* **2011**, *32*, 1456–1465. doi:10.1002/jcc.21759.
43. Grimme S., Antony J., Ehrlich S., Krieg H. *J. Chem. Phys.* **2010**, *132*, 154104. doi:10.1063/1.3382344.

44. Weigend F., Ahlrichs R. *Phys. Chem. Chem. Phys.* **2005**, *7*, 3297. doi:10.1039/b508541a.

45. Kruse H., Grimme S. *J. Chem. Phys.* **2012**, *136*, 154101. doi:10.1063/1.3700154.

46. Weigend F. *Phys. Chem. Chem. Phys.* **2006**, *8*, 1057–1065. doi:10.1039/b515623h.

47. Eichkorn K., Treutler O., Öhm H., Häser M., Ahlrichs R. *Chem. Phys. Lett.*, **1995**, *242*, 652–660. doi: 10.1016/0009-2614(95)00838-U.

48. Jmol: an open-source Java viewer for chemical structures in 3D. http://www.jmol.org/ Accessed date: July 23, 2021.

49. Assaba I.M., Rahali S., Belhocine Y., Allal H. *J. Mol. Struct.* **2021**, *1227*, 129696. doi:10.1016/j.molstruc.2020.129696.

50. Belhocine Y., Bouhadiba A., Rahim M., Nouar L., Djilani I., Khatmi D-E. *Macroheterocycles* **2018**, *11*, 203–209. doi:10.6060/mhc170829b.

51. de Sousa F.B., Leite Denadai A.M., Lula I.S., Nascimento Jr C.S., Fernandes Neto N.S.G., Lima A.C., de Almeida W.B., Sinisterra R.D. *J. Am. Chem. Soc.* **2008**, *130*, 8426–8436. doi:10.1021/ja801080v.

52. Venkatesh G., Sivasankar T., Karthick M. Rajendiran N. *J. Incl. Phenom. Macrocycl. Chem.* **2013**, *77*, 309–318. doi:10.1007/s10847-012-0248-z.

53. Ammouchi N., Allal H., Belhocine Y., Bettaz S., Zouaoui E. *J. Mol. Liq.* **2020**, *300*, 133–145. doi:10.1016/j.molliq.2019.112309.

54. Elistratova M.A., Zakharova I.B., Kvyatkovskii O.E. *Macroheterocycles* **2019**, *12*, 370–374. doi:10.6060/mhc190552e.

55. Fifere A., Marangoci N., Maier S., Coroaba A., Maftei D., Pinteala M. *Beilstein J. Org. Chem.* **2012**, *8*, 2191–2201. doi:10.3762/bjoc.8.247.

56. Nagarajan V., Chandiramouli R. *Appl. Surf. Sci.* **2015**, *344*, 65–78. doi:10.1016/j.apsusc.2015.03.069.

57. Allal H., Belhocine Y., Rahali S., Damous M., Ammouchi N. *J. Mol. Model.* **2020**, *26*, 128. doi:10.1007/s00894-020-04388-3.

58. Contreras-García J., Boto R.A., Izquierdo-Ruiz F., Reva I., Woller T., Alonso M. *Theor. Chem. Acc.* **2016**, *135*, 242. doi:10.1007/s00214-016-1977-7.

59. Saleh G., Gatti C., Presti L.L. *Comput. Theor. Chem.* **2012**, *998*, 148–163. doi:10.1016/j.comptc.2012.07.014.

60. Lefebvre C., Rubez G., Khartabil H., Boisson J.C., Contreras-García J., Hénon E. *Phys. Chem. Chem. Phys.* **2017**, *19*, 17928–17936. doi:10.1039/c7cp02110k.

61. Lu T., Chen F. *J. Comput. Chem.* **2012**, *33*, 580–592. doi:10.1002/jcc.22885.

62. Humphrey W., Dalke A., Schulten K. *J. Mol. Graph.* **1996**, *14*, 33–38. doi:10.1016/0263-7855(96)00018-5.